

Modeling thermionic emission from laser-heated nanoparticles

J. M. Mitrani,^{1,a)} M. N. Shneider,² B. C. Stratton,¹ and Y. Raitses¹

¹Princeton Plasma Physics Laboratory, Princeton, New Jersey 08540, USA

²Department of Mechanical Engineering, Princeton University, Princeton, New Jersey 08544, USA

(Received 17 November 2015; accepted 18 January 2016; published online 1 February 2016)

An adjusted form of thermionic emission is applied to calculate emitted current from laser-heated nanoparticles and to interpret time-resolved laser-induced incandescence (TR-LII) signals. This adjusted form of thermionic emission predicts significantly lower values of emitted current compared to the commonly used Richardson-Dushman equation, since the buildup of positive charge in a laser-heated nanoparticle increases the energy barrier for further emission of electrons. Thermionic emission influences the particle's energy balance equation, which can influence TR-LII signals. Additionally, reports suggest that thermionic emission can induce disintegration of nanoparticle aggregates when the electrostatic Coulomb repulsion energy between two positively charged primary particles is greater than the van der Waals bond energy. Since the presence and size of aggregates strongly influences the particle's energy balance equation, using an appropriate form of thermionic emission to calculate emitted current may improve interpretation of TR-LII signals. © 2016 AIP Publishing LLC. [<http://dx.doi.org/10.1063/1.4940992>]

The laser-induced incandescence (LII) diagnostic has been extensively applied (Ref. 1, and references therein) as a combustion diagnostic for minimally invasive, *in situ* characterization of soot particles in background flame environments. The LII diagnostic has also been used to characterize carbon black² and to study gas-phase synthesis of non-carbonaceous nanoparticles.^{3–5} For time-resolved LII (TR-LII), particles are typically heated with a short-pulsed laser, and the induced incandescence signals are subsequently recorded. Since incandescence is a function of particle temperature, $T(t)$, interpreting TR-LII signals involves calculating $T(t)$ by numerically solving the particles' mass and energy balance equations during and after the laser pulse. The mass and energy balance equations describe the influence of various heat transfer processes on $T(t)$.

One of the heat transfer processes is thermionic emission, which describes the release of electrons from hot cathodes. Richardson first proposed⁶ that the relationship between thermionic emission current and cathode temperature follow an Arrhenius equation. Subsequent research led to the well-known Richardson-Dushman equation

$$J_{RD} = A_0 T^2 \exp\left(-\frac{\phi}{k_B T}\right), \quad (1)$$

where J_{RD} is the emitted current density (A/cm^2), T is the cathode temperature, ϕ is the cathode work function, and $A_0 = 4\pi m_e k_B^2 e / h^3 \sim 120 \text{ A}/\text{cm}^2 \text{ K}^2$ is the Richardson constant, where m_e , k_B , e , and h are the electron mass, Boltzmann's constant, electron charge, and Planck's constant, respectively. Although thermionic emission has been traditionally applied to characterize current emitted from hot metal filaments (e.g., gas discharge lamps), thermionic emission can also describe current emitted from any hot conducting particles, such as laser-heated nanoparticles. Consequently, thermionic emission will influence interpretation of TR-LII signals when the heat

loss is significant, with respect to other heat loss mechanisms in the energy balance equation.

Thermionic emission can influence the particle's energy balance equation by directly cooling the particle,^{7,8} and by inducing disintegration of nanoparticle aggregates.⁹ The particle cooling rate due to thermionic emission has^{7,8} been previously described by a modified form of the Richardson-Dushman equation, $Q_{RD} = (\pi D^2 \phi / e) J_{RD}$, where Q_{RD} (J/s) is the particle cooling rate, and D is the primary particle diameter. Filippov *et al.*⁹ described a model where thermionic emission of electrons results in a positive charge buildup in the primary particles, which in turn can induce disintegration of nanoparticle aggregates when the electrostatic Coulomb repulsion energy between positively charged particles is greater than the van der Waals bond energy. This phenomenon of laser-induced aggregate disintegration is qualitatively similar to a Coulomb explosion,¹⁰ where ultrafast picosecond or femtosecond lasers with high instantaneous intensities (typically greater than $10^{14} \text{ W}/\text{cm}^2$) are used to irradiate atomic or molecular clusters. The high laser intensities quickly ionize the cluster, which subsequently “explodes” when the ions rapidly separate. Production of X-rays^{11,12} and high-velocity ($>100 \text{ keV}$) ions^{13–15} has been observed from heating noble gas clusters with intense pulses from femtosecond lasers. Since recent results^{16–20} show that aggregation significantly influences TR-LII signals by reducing the conductive cooling rate, appropriately modeling thermionic emission should be considered when interpreting TR-LII signals.

When applied to laser-heated nanoparticles, the Richardson-Dushman equation (Equation (1)) significantly overestimates the emitted current, and consequently, the particle cooling rate. Thermionic emission from a laser-heated nanoparticle results in a positive charge buildup, which increases the barrier for subsequent emission of electrons. (The positive charge buildup in a traditional case of thermionic emission from a metal filament in a gas discharge lamp

^{a)}Electronic mail: jmitrani@pppl.gov

is negligible as long as current is being supplied to the filament.) Therefore, the Richardson-Dushman equation should be adjusted to include the effects of the positive charge buildup, resulting in the following expression:²¹

$$J_{Therm} = A_0 T^2 \exp\left(-\frac{(\phi + \Delta\phi)}{k_B T}\right), \quad (2)$$

where J_{Therm} describes the adjusted current density (A/cm²) for thermionic emission from laser-heated particles, and $\Delta\phi$ describes the increased barrier (eV) for further electron emission due to the positive charge buildup. For a spherical particle with diameter D and charge $q_p > 0$, $\Delta\phi$ has the following form:

$$\Delta\phi = eV_P = k_E \frac{eq_p}{R}, \quad (3)$$

where $V_P = q_p/C_P$ is the electric potential, $C_P = (4\pi\epsilon_0)R$ is the capacitance, $R \equiv D/2$ is the radius, and $k_E \equiv 1/(4\pi\epsilon_0)$ is the Coulomb constant. Equation (3) reflects the electrostatic Coulomb barrier at the particle surface for emitted electrons. The particle charge, q_p , is equal to the outgoing charge of emitted electrons and can be calculated by integrating current (Equation (2)) with respect to time

$$q_p(t) = eN_{Emi}(t) = \pi D^2 \int_0^t J_{Therm}(s) ds, \quad (4)$$

assuming isotropic current emission, where $N_{Emi}(t)$ is the number of emitted electrons.

Since the LII diagnostic is most developed for studying soot particles in background flame environments, thermionic emission current was calculated under those conditions. The laser fluence, gas temperature, and initial particle diameter were set to 0.2 J/cm², 1800 K, and 30 nm, respectively. Figure 1 shows that thermionic emission current is significantly reduced when effects of the particle's positive charge buildup, $\Delta\phi$ (Equation (3)), are included. Soot temperature, $T(t)$, was calculated by numerically solving mass and energy balance equations

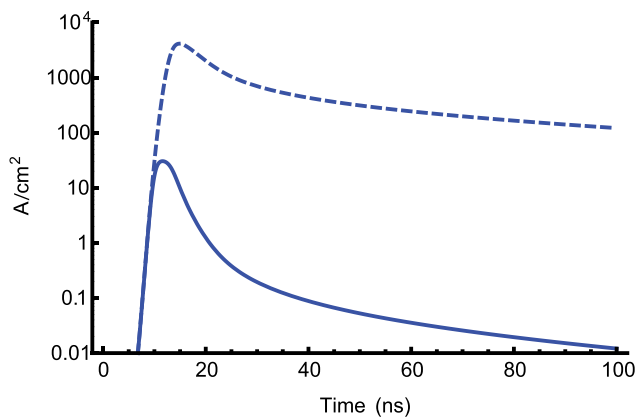


FIG. 1. Predicted current density using the standard (Equation (1), dashed line) and adjusted (Equation (2), solid line) form of the Richardson-Dushman equation. The adjusted form includes the effects of positive charge buildup in the nanoparticle, resulting in a sharp decrease in the predicted current density.

$$\frac{dU_{Int}}{dt} = Q_{Abs} - Q_{Rad} - Q_{Cond} - Q_{Sub} - Q_{Therm}, \quad (5a)$$

$$\frac{dM}{dt} = \dot{M}_{Sub}, \quad (5b)$$

where the U_{Int} is the nanoparticle's internal energy²² and is proportional to particle temperature, $T(t)$. The Q_i (J/s) terms are plotted in Figure 2 and describe the rate of energy gained or lost by absorption of laser energy (Rayleigh approximation for absorption^{16,18,23}), Q_{Abs} ; blackbody radiation,²⁴ Q_{Rad} ; conductive cooling (McCoy and Cha model²⁵), Q_{Cond} ; sublimation, Q_{Sub} ; and thermionic emission, $Q_{Therm} = ((\phi + \Delta\phi)\pi D^2/e)J_{Therm}$ (Equation (2)). The work function of graphite is $\phi = 4.7$ eV, which was used to calculate Q_{Therm} . Particle mass loss, \dot{M}_{Sub} (g/s), is primarily caused by sublimation of C₁–C₅ clusters and was calculated using the temperature dependent values^{7,26} for the average partial pressures, enthalpies of formation, and molecular weights of the sublimed species. Figure 2 shows that thermionic emission has a negligible influence on the particles' mass and energy balance equations when effects of the positive charge buildup, $\Delta\phi$, are included. Although there is significant disagreement about values of specific terms used in the mass and energy balance equations (Ref. 7, and references therein), the results shown in Figure 2 remain valid: including effects of $\Delta\phi$ causes particle cooling from thermionic emission to become insignificant with respect to other cooling terms in the energy balance equation (Equation (5a)).

The number of emitted electrons was calculated from Equation (4) and is shown in Figure 3. The predicted electric potential (Equation (3)) at the nanoparticle surface is 2.5 V. For comparison, the work function of graphite is 4.7 eV.

Following the approach by Filippov *et al.*,⁹ laser-induced disintegration of nanoparticle aggregates may be predicted to occur for given experimental conditions, even with the lower values of emitted current calculated from the adjusted form of thermionic emission. Thermionic emission of electrons results in positively charged nanoparticles.

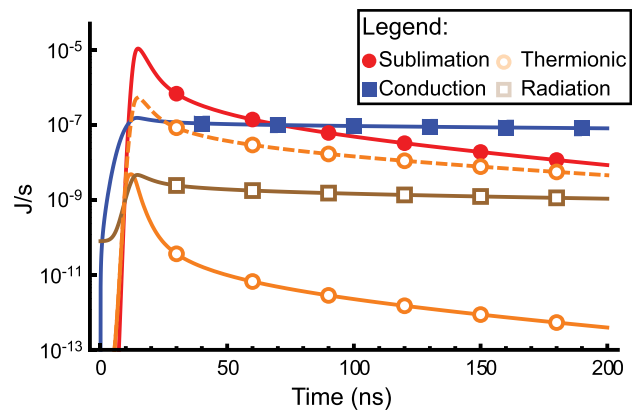


FIG. 2. Relative magnitudes of the relevant heat transfer processes: sublimation, Q_{Sub} (solid red circles), thermal conduction, Q_{Cond} (solid blue squares), thermionic emission, Q_{Therm} (hollow orange circles), and radiation, Q_{Rad} (hollow brown squares). Thermionic emission was calculated with (Equation (2), solid line) and without (Equation (1), dashed line) including the influence of the positive charge buildup, $\Delta\phi$. Including $\Delta\phi$ results in Q_{Therm} having an insignificant effect on the energy balance equation, with respect to other heat transfer processes shown above.

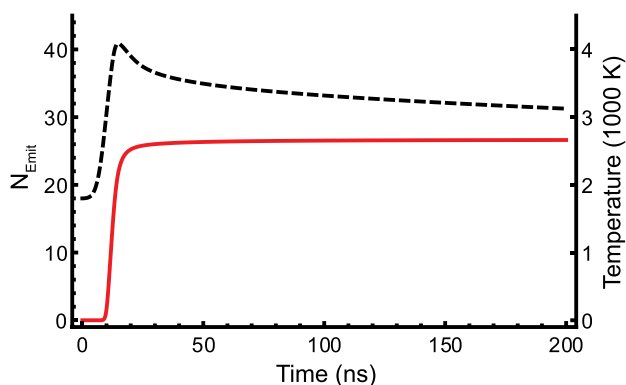


FIG. 3. Predicted temporal profiles for cumulative number of emitted electrons, $N_{Emit}(t)$ (red, solid line), and particle temperature, $T(t)$ (black, dashed line). Equation (4) was used to calculate $N_{Emit}(t)$, and the mass and energy balance equations (Equation (5)) were numerically solved, to predict $T(t)$. The timescale for emission of current is ~ 10 – 20 ns.

When the electrostatic Coulomb repulsion energy between positively charged particles is greater than the van der Waals bond energy, the nanoparticle aggregate can disintegrate into primary particles. Assuming a monodisperse diameter distribution within an aggregate, the repulsion energy between two charged spheres is

$$U_{Rep} = k_E \frac{(eN_{Emit})^2}{D + d}, \quad (6)$$

where $U_{Rep} = \sim 33$ eV, N_{Emit} was calculated from Figure 3, and $d = 0.7$ nm was assumed to be the van der Waals bond distance. The van der Waals bond energy between two spheres with diameters much greater than the van der Waals bond length, $D \gg d$, is²⁷

$$U_{VDW} = \frac{A_H D}{24d}, \quad (7)$$

where $U_{VDW} = 5.2$ eV is the van der Waals bond energy, and $A_H = 2.9$ eV is the Hamaker constant for graphite.^{28,29} For comparison, similarly sized carbonaceous nanoparticle aggregates are predicted to disintegrate when $N_{Emit} = 11$ electrons, well under the predicted values for N_{Emit} shown in Figure 3. Note that this approach assumes uniform aggregate heating, consistent with Rayleigh-Debye-Gans polydisperse fractal aggregate (RDG/PFA) theory,^{30–32} and uniform thermionic emission within an aggregate. For simplicity, disintegration of nanoparticle aggregates was assumed to be a binary process. The contribution of laser-induced oxidation to the particle's energy balance equation was assumed to be insignificant.²²

The above calculation assumes that all primary particles within a nanoparticle aggregate are connected by van der Waals bonds. The combustion-generated soot aggregates consist of primary particles joined by covalent or other chemical bonds,³³ including bridging between primary particles.²⁰ Studies^{33,34,36} suggest that although laser pulses may induce partial disintegration of large soot aggregates into smaller soot aggregates, laser-induced graphitization will strengthen chemical bonds between primary particles and prevent complete disintegration of soot aggregates into primary particles. However, the laser-induced disintegration

of soot aggregates has been reported under high vacuum conditions.³⁷ Unlike soot, other aggregates of less amorphous nanoparticles, such as carbon fullerenes^{38,39} and metal oxide^{40,41} nanoparticles, consist of primary particles joined by van der Waals bonds. Consequently, an appropriate treatment of laser-induced aggregate disintegration should be considered for LII studies involving nanoparticle aggregates.

An additional factor which can prevent laser-induced disintegration of nanoparticle aggregates involves emitted electrons returning to the partially positively charged nanoparticle aggregate. Figure 3 shows that the timescale for current emission is ~ 10 – 20 ns. The timescale for electron attachment to molecular oxygen (forming O_2^-) in room temperature, atmospheric pressure air was measured to be ~ 12 ns,³⁵ which is similar to the predicted emission time. Under this assumption, almost all emitted electrons will attach to O_2 molecules and will not return to partially positively charged nanoparticles. Other factors which can prevent electrons from returning are high vacuum conditions, strong external electric fields, or the presence of a background plasma. In the presence of a background plasma, since nanoparticles typically acquire negative charge, particle cooling due to thermionic emission is predicted to be more significant. The ponderomotive energy of electrons in the laser-generated electric field is trivial for laser fluences (< 1 J/cm²) and pulse durations (~ 10 ns) typically used for LII experiments. If the emitted electrons do not return to the nanoparticle aggregate, then the nanoparticles will remain positively charged, which can lead to aggregate disintegration.

In summary, an adjusted form of thermionic emission (Equation (2)) for laser-heated nanoparticles, which incorporates the effects of the particles' positive charge buildup, is presented. The buildup of positive charge results in significantly lower values of the thermionic emission current. Nevertheless, even with the lower values of current calculated from the adjusted form of thermionic emission (Equation (2)), the laser-induced disintegration of nanoparticle aggregates can still occur. Appropriately modeling thermionic emission from laser heated nanoparticles is essential for predicting the likelihood of laser-induced disintegration of nanoparticle aggregates and may improve interpretation of TR-LII signals.

This work was supported by the U.S. Department of Energy, Office of Science, Basic Energy Sciences, Materials Sciences and Engineering Division. James M. Mitrani acknowledges the support from the Program in Plasma Science and Technology, at the Princeton Plasma Physics Laboratory.

¹C. Schulz, B. F. Kock, M. Hofmann, H. Michelsen, S. Will, B. Bougie, R. Sultz, and G. Smallwood, *Appl. Phys. B* **83**, 333 (2006).

²N. Moteki and Y. Kondo, *Aerosol Sci. Technol.* **41**, 398 (2007).

³T. Sipkens, R. Mansmann, K. Daun, N. Petermann, J. Titantah, M. Karttunen, H. Wiggers, T. Dreier, and C. Schulz, *Appl. Phys. B* **116**, 623 (2014).

⁴T. Sipkens, N. Singh, K. Daun, N. Bizmark, and M. Ioannidis, *Appl. Phys. B* **119**, 561 (2015).

⁵F. Cignoli, C. Bellomunno, S. Maffi, and G. Zizak, *Appl. Phys. B* **96**, 593 (2009).

- ⁶O. W. Richardson, in *Proceedings of the Cambridge Philosophical Society: Mathematical and Physical Sciences* (University Press, 1901), Vol. 11, pp. 286–295.
- ⁷H. Michelsen, F. Liu, B. F. Kock, H. Bladh, A. Boiarciuc, M. Charwath, T. Dreier, R. Hedef, M. Hofmann, J. Reimann, S. Will, P. Bengtsson, H. Bockhorn, F. Foucher, K. Geigle, C. Mounaim-Rousselle, C. Schulz, R. Stirn, B. Tribalet, and R. Suntz, *Appl. Phys. B* **87**, 503 (2007).
- ⁸K. McManus, J. Frank, M. Allen, and W. Rawlins, “Characterization of laser-heated soot particles using optical pyrometry,” in *36th AIAA Aerospace Sciences Meeting and Exhibit, Aerospace Sciences Meetings* (1998), AIAA-98-0159.
- ⁹A. Filippov, M. Markus, and P. Roth, *J. Aerosol Sci.* **30**, 71 (1999).
- ¹⁰K. Sattler, J. Mühlbach, O. Echt, P. Pfau, and E. Recknagel, *Phys. Rev. Lett.* **47**, 160 (1981).
- ¹¹A. Borisov, A. McPherson, K. Boyer, and C. Rhodes, *J. Phys. B: At., Mol. Opt. Phys.* **29**, L113 (1996).
- ¹²S. Dobosz, M. Lezius, M. Schmidt, P. Meynadier, M. Perdrix, D. Normand, J.-P. Rozet, and D. Vernhet, *Phys. Rev. A* **56**, R2526 (1997).
- ¹³T. Ditmire, J. G. Tisch, E. Springate, M. Mason, N. Hay, R. Smith, J. Marangos, and M. Hutchinson, *Nature* **386**, 54 (1997).
- ¹⁴T. Ditmire, J. Tisch, E. Springate, M. Mason, N. Hay, J. Marangos, and M. Hutchinson, *Phys. Rev. Lett.* **78**, 2732 (1997).
- ¹⁵M. Lezius, S. Dobosz, D. Normand, and M. Schmidt, *Phys. Rev. Lett.* **80**, 261 (1998).
- ¹⁶F. Liu, M. Yang, F. A. Hill, D. R. Snelling, and G. J. Smallwood, *Appl. Phys. B* **83**, 383 (2006).
- ¹⁷F. Liu, G. J. Smallwood, and D. R. Snelling, *J. Quant. Spectrosc. Radiat. Transfer* **93**, 301 (2005).
- ¹⁸D. R. Snelling, F. Liu, G. J. Smallwood, and Ö. L. Gülder, *Combust. Flame* **136**, 180 (2004).
- ¹⁹H. Bladh, J. Johnsson, J. Rissler, H. Abdulhamid, N.-E. Olofsson, M. Sanati, J. Pagels, and P.-E. Bengtsson, *Appl. Phys. B* **104**, 331 (2011).
- ²⁰J. Johnsson, H. Bladh, N.-E. Olofsson, and P.-E. Bengtsson, *Appl. Phys. B* **112**, 321 (2013).
- ²¹M. N. Shneider, *Phys. Plasmas* **22**, 073303 (2015).
- ²²H. A. Michelsen, *J. Chem. Phys.* **118**, 7012 (2003).
- ²³C. F. Bohren and D. R. Huffman, *Absorption and Scattering of Light by Small Particles* (John Wiley & Sons, 1983).
- ²⁴H. Bladh, J. Johnsson, and P.-E. Bengtsson, *Appl. Phys. B* **90**, 109 (2008).
- ²⁵B. McCoy and C. Cha, *Chem. Eng. Sci.* **29**, 381 (1974).
- ²⁶H. Leider, O. Krikorian, and D. Young, *Carbon* **11**, 555 (1973).
- ²⁷H. Hamaker, *Physica* **4**, 1058 (1937).
- ²⁸J. Visser, *Adv. Colloid Interface Sci.* **3**, 331 (1972).
- ²⁹F. O. Goodman and N. Garcia, *Phys. Rev. B* **43**, 4728 (1991).
- ³⁰G. W. Mulholland and R. D. Mountain, *Combust. Flame* **119**, 56 (1999).
- ³¹T. L. Farias, Ü. Ö. Köylü, and M. G. Carvalho, *Appl. Opt.* **35**, 6560 (1996).
- ³²U. O. Koylu and G. Faeth, *J. Heat Transfer* **116**, 971 (1994).
- ³³H. A. Michelsen, A. V. Tivanski, M. K. Gilles, L. H. van Poppel, M. A. Dansson, and P. R. Buseck, *Appl. Opt.* **46**, 959 (2007).
- ³⁴R. L. Vander Wal, T. Ticich, and A. Stephens, *Appl. Phys. B* **67**, 115 (1998).
- ³⁵A. Dogariu, M. N. Shneider, and R. B. Miles, *Appl. Phys. Lett.* **103**, 224102 (2013).
- ³⁶S. De Iuliis, F. Cignoli, S. Maffi, and G. Zizak, *Appl. Phys. B* **104**, 321 (2011).
- ³⁷V. Beyer and D. Greenhalgh, *Appl. Phys. B* **83**, 455 (2006).
- ³⁸J. L. Atwood, L. J. Barbour, M. W. Heaven, and C. L. Raston, *Angewandte Chemie* **115**, 3376 (2003).
- ³⁹B. Bhushan, B. Gupta, G. W. Van Cleef, C. Capp, and J. V. Coe, *Appl. Phys. Lett.* **62**, 3253 (1993).
- ⁴⁰Y. Lalatonne, J. Richardi, and M. Pileni, *Nature Materials* **3**, 121 (2004).
- ⁴¹S. K. Friedlander, H. D. Jang, and K. H. Ryu, *Appl. Phys. Lett.* **72**, 173 (1998).